ETH BIBLIOTHEK

ETH-BIB - Bestellschein ETH-BIB:000001256871

Bestellart: Normal

Lieferformat: PDF Lieferweg: EMAIL

Eingang: 2016-12-02 15:55:13 Lieferung bis: 2016-12-07 15:55:13

Kundennummer: K000003517 Bestellnummer: E001302783

Angaben zum bestellten Dokument:

Signatur:	**P N 23 88 (2012) 1/6 ETH-HDB (Zuerich) K6**
Zeitschriftentitel:	International journal of radiation biology covering the phy
Band/Heft::	
Erscheinungsjahr:	
Seiten:	164-170
Autor:	McNamara AL1, Guatelli S, Prokopovich D
Artikel:	A comparison of X-ray and proton beam low energy
ISSN:	

Bemerkung zum Dokument: 88/2012- Issue 1-2

Angaben zum Kunden

Adresse CH - 1211 Geneve 23

Kontaktperson: . lib.acq@cern.ch

Kundennummer: E-13519

Kundennummer:

Bestellnummer

Bearbeitungsvermerk

International Journal of Radiation Biology, January–February 2012; 88(1–2): 164–170

ISSN 0955-3002 print / ISSN 1362-3095 online
DOI: 10.3109/09553002.2011.627975

informa
healthcare

A comparison of X-ray and proton beam low energy secondary electron track structures using the low energy models of Geant4

Aimee L. McNamara[1], Susanna Guatelli[2], Dale A. Prokopovich[1], Mark I. Reinhard[1] & Anatoly B. Rosenfeld[2]

[1]*Australian Nuclear Science and Technology Organisation (ANSTO), Lucas Heights, NSW, and* [2]*Centre for Medical Radiation Physics (CMRP), University of Wollongong, NSW, Australia*

Abstract

Purpose: **Lethal cell damage by ionising radiation is generally initiated by the formation of complex strand breaks, resulting from ionisation clusters in the DNA molecule. A better understanding of the effect of the distribution of ionisation clusters within the cell and particularly in regard to DNA segments could be beneficial to radiation therapy treatment planning. Low energy X-rays generate an abundance of low energy electrons similar to that associated with MeV protons. The study and comparison of the track structure of photon and proton beams could permit the substitution of photon microbeams for single cell ion irradiations at proton facilities used to predict the relative biological effectiveness (RBE) of charged particle fields.** ***Materials and methods:*** **The track structure of X-ray photons is compared with proton pencil beams in voxels of approximate DNA strand size (2 × 2 × 5 nm). The Very Low Energy extension models of the Monte Carlo simulation toolkit GEometry ANd Tracking 4 (Geant4) is used. Simulations were performed in a water phantom for an X-ray and proton beam of energies 100 keV and 20 MeV, respectively.** ***Results:*** **The track structure of the photon and proton beams are evaluated using the ionisation cluster size distribution as well as the radial dose deposition of the beam.** ***Conclusions:*** **A comparative analysis of the ionisation cluster distribution and radial dose deposition obtained is presented, which suggest that low energy X-rays could produce similar ionisation cluster distributions to MeV protons on the DNA scale of size at depths greater than ~10 μm and at distances greater than ~1 μm from the beam centre. Here the ionisation cluster size for each beam is less than ~100. The radial dose deposition is also approximately equal at large depths and at distances greater than 10 μm from the beam centre.**

Keywords: Ionising radiation, DNA damage, Geant4, track structure

Introduction

Lethal damage to cells by ionising radiation is generally instigated by the initial damage to the DNA molecule, in the form of complex single- or double-strand breaks. Since multiple ionisations produced within sites of 2–3 nm correlate well with yields observed for double-strand breaks (Brenner and Ward 1992), the specific number of ionisations (defined as the ionisation cluster size) and the distribution of such clusters within the DNA segment, i.e., the ionisation clustering distribution associated with the absorbed radiation is a particularly important factor in estimating damage. Monte Carlo simulations have shown that ionisation clustering can be correlated with the biological effectiveness of radiation on the nanometre scale (see e.g., Friedland et al. 1998, Nikjoo et al. 1999) and may be a more pertinent quantity than the absorbed dose in describing radiation damage.

The low-energy secondary electrons, produced through the interaction of ionising radiation with matter, play a significant role in the production of ionising events. Simulation of photon or proton beams provide evidence that delta electrons with energies less than 1 keV can produce approximately 50% of all ionisations (Nikjoo and Goodhead 1991). Low energy electrons have a greater probability of producing ionisations on the nanometre scale than high energy electrons. This can be explained in terms of the linear energy transfer (LET) which increases with decreasing electron energy. Electrons with energies less than 10 keV are more likely to have a higher biological effectiveness through the formation of larger ionisation clusters, which can result in a greater fraction of double-strand breaks compared to single-strand breaks in DNA. We investigate these effects in an effort to evaluate the ionisation cluster distribution and dose deposition of low energy X-rays, as those found in microbeam radiation therapy (Siegbahn et al. 2006, Spiga et al. 2007), as well as 10–50 MeV protons found in abundance in the Bragg peak of proton therapy (see Miller 1995 and Olsen et al. 2007 for reviews) on the micrometer to nanometre scale. The track structure of a monoenergetic photon and proton pencil beam in liquid water is compared on the nanometre scale using the Monte Carlo simulation toolkit GEometry ANd Tracking 4 (Geant4). In particular, the ionisation cluster distribution of each particle type is compared.

Correspondence: Dr Aimee McNamara, PhD, Locked Bag 2001, Kirrawee DC, NSW, 2232, Australia. Tel: + 61 02 9717 7236. Fax: + 61 02 9717 7250. E-mail: aimee.mcnamara@ansto.gov.au.

(Received 19 December 2010; revised 1 September 2011; accepted 23 September 2011)

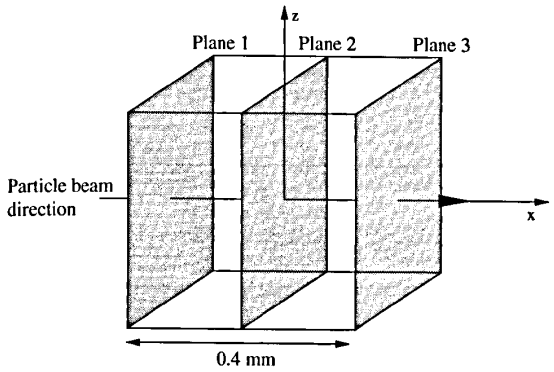

Figure 1. Illustration of the simulation geometry. Beam is incident on a water-filled cube of dimension 0.4 mm. The properties of each particle type are assessed on the nanometre scale at three different positions along the beam path: At a depth of 0 mm (plane 1), 0.2 mm (plane 2) and 0.4 mm (plane 3) in the phantom.

If it can be shown that the ionisation cluster distributions are similar, the substitution or supplementation of photon microbeams for protons in targeted single cell irradiations could be feasible. In this paper we also investigate the radial dose distribution for completeness.

Materials and methods

The open-source, general-purpose Monte Carlo simulation toolkit Geant4 Version 9.3 (Agostinelli et al. 2003, Allison et al. 2006) was used for the investigation. Nanodosimetric capabilities are enabled by the Geant4 Very Low Energy physics models (Geant4-DNA extension), which allow detailed simulation of interactions of electrons in liquid water down to energies of a few eV (Chauvie et al. 2006, Incerti et al. 2009).

In the Geant4 application two different monoenergetic radiation types were simulated: X-rays and protons both incident on a liquid water cube with dimension 0.4 mm (see Figure 1). Both incident particles were modelled as pencil beams with zero width. For this preliminary investigation we assessed the ionisation clustering distribution of each beam type on the nanometre scale for approximately 20 cell lengths (assuming average cell length ~ 20 μm). This simulation set-up was designed to model a cell layer for radiobiological experiments. Simulations were carried out for a range of incident photon and proton energies used in microbeam radiation therapy and proton therapy; here results for 100 keV primary photons and 20 MeV protons are presented, typical of particle energies used in these modalities.

To model photon interactions the Geant4 Low Energy Electromagnetic Package (based on the Livermore evaluated data libraries) was activated, including the photoelectric effect, Compton scattering, Rayleigh scattering and pair production, valid down to 250 eV. For protons with $E > 10$ MeV the Low Energy Package models were used, including ionisation and multiple scattering. The hadronic processes (inelastic and elastic scattering) were additionally activated. The Low Energy Package models were similarly activated for secondary electrons with $E > 10$ keV, including ionisation, bremsstrahlung and multiple scattering.

Protons and electrons with energies lower than 10 MeV and 10 keV, respectively were transported in the water medium down to a few eV, using the Very Low Energy extensions. Electron ionisation, excitation and elastic scattering (Champion elastic model) were included. The lower energy limit for the excitation and elastic scattering models was set to 8.23 eV (Chauvie et al. 2007a, Champion et al. 2009). The physics processes of the low energy protons (< 10 MeV) included charge decrease, excitation and ionisation from the Very Low Energy models (Chauvie et al. 2007a, 2007b).

Modelling DNA segments and nucleosomes as nanometric volumes, e.g., cylinders, is a common practice in nanodosimetric simulations and has been shown to be sufficient in modelling the essential aspects of the radiation effects on DNA segments (Nikjoo et al. 1997). In this work, the phantom was parameterised into rectangular DNA strand sized volumes of dimension $5 \times 2 \times 2$ nm in order to assess the formation of ionisations in the entire volume. The rectangular volumes chosen have the same approximate dimensions as cylindrical volumes used in similar studies, but allow all ionisations in the phantom to be accounted for. Since this study consists of a relative comparison of the track structure of photons and protons, the choice of nanometric geometry should not affect the results of the study.

The simulation produces the number of ionisations in each voxel (cluster size distribution) and the radial dose distribution. The ionisation cluster distribution has been shown to be pertinent in characterising the track structure (Nikjoo et al. 1998), and is used to compare the proton and photon pencil beams.

Results

An X-ray and proton monenergetic pencil beam incident on a water cube was simulated for initial primary photon and proton energies of 100 keV and 20 MeV, respectively (Figures 2 and 3). The number of ionisations occurring within nanometric voxels (the cluster size distribution), with dimension $5 \times 2 \times 2$ nm, was recorded at the start (plane 1), middle (plane 2) and end (plane 3) of the beam trajectory path through the phantom (see Figure 1). Results are plotted for projections on the YZ plane with the beam axis centred on (0, 0) for three different depths in the water phantom: 0.0 mm, 0.2 mm and 0.4 mm (a, b and c plots of Figures 2 and 3, respectively). The colour axis in Figures 2 and 3 represent the number of ionisations per voxel. Figure 4 shows the cluster distribution in planes 1, 2 and 3 for photons and protons in the y-plane up to 10^5 nm from the beam centre. In order to compare the ionisation clustering, 1.0×10^8 incident photons and 2.0×10^4 incident protons were simulated to produce approximately the same overall number of ionisations (~ 2.5×10^6) in the entire phantom volume.

The radial dose distribution at three different positions along the 100 keV X-ray and 20 MeV proton pencil beam is plotted in Figure 5. The dose distribution in planes 1, 2 and 3 (see Figure 1) are calculated in concentric rings of radius r (radial distance from beam axis) and thickness 2 μm.

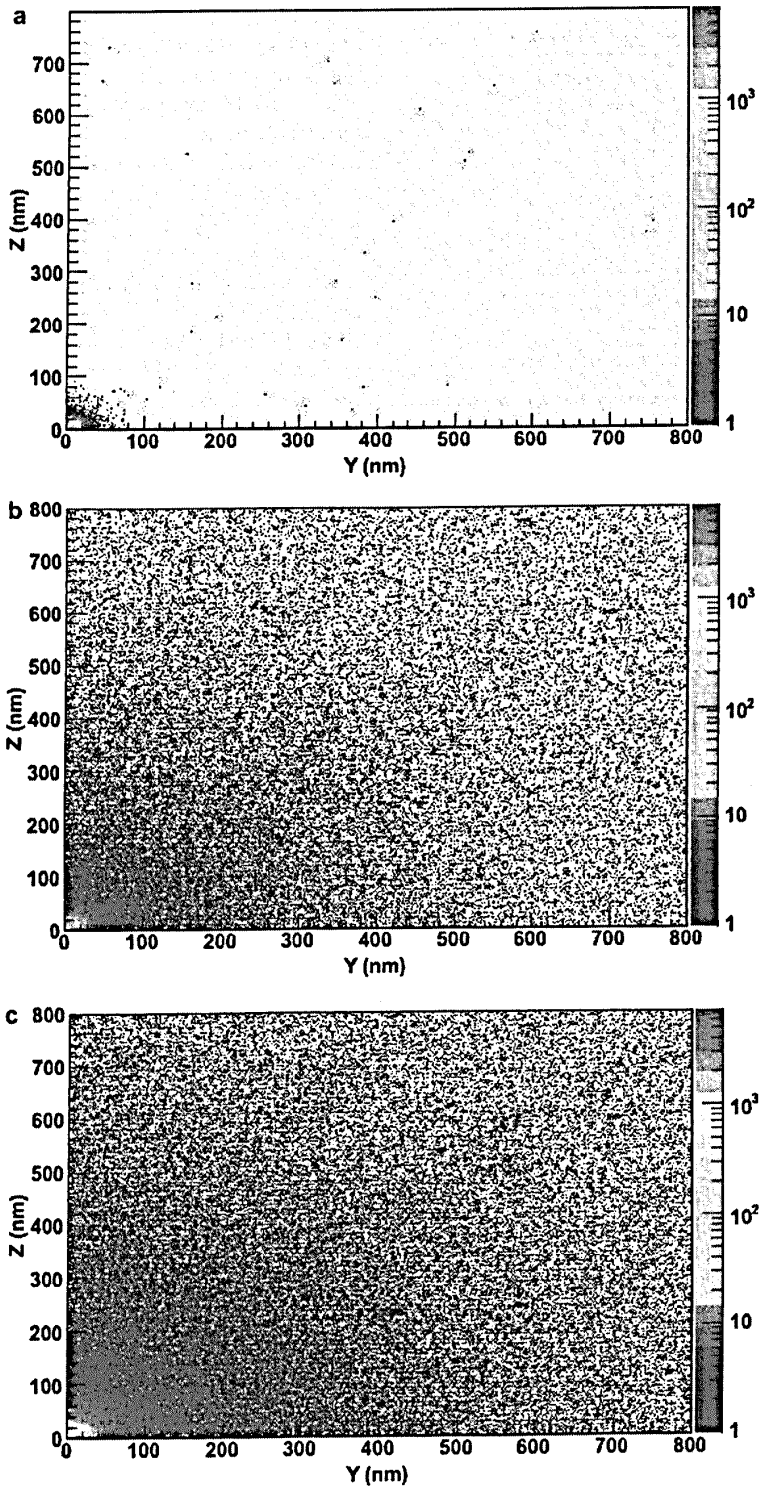

Figure 2. The distribution of ionisation clusters at different points along the trajectory of a 100 keV X-ray pencil beam in the YZ plane, for slices of thickness 5 nm, for 10^8 primary photons. The colour scale on the right of each plot indicates the ionisation cluster size (number of ionisations per voxel). The beam is centred on (0,0). The top plot is for a depth of 0.0 mm in the water phantom and the middle and bottom plots are for depths 0.2 mm and 0.4 mm, respectively.

Discussion

The ionisation cluster distributions of a 100 keV X-ray and 20 MeV proton pencil beam are compared on the nanometre scale at different points along the beam path in a liquid water cube phantom.

A single proton produces an overall higher number of ionisations than a single photon. In the simulation geometry considered, approximately 5000 photons are required to produce the same total amount of ionisations as a single proton. In each simulated case, ~10^6 ionisations are produced in

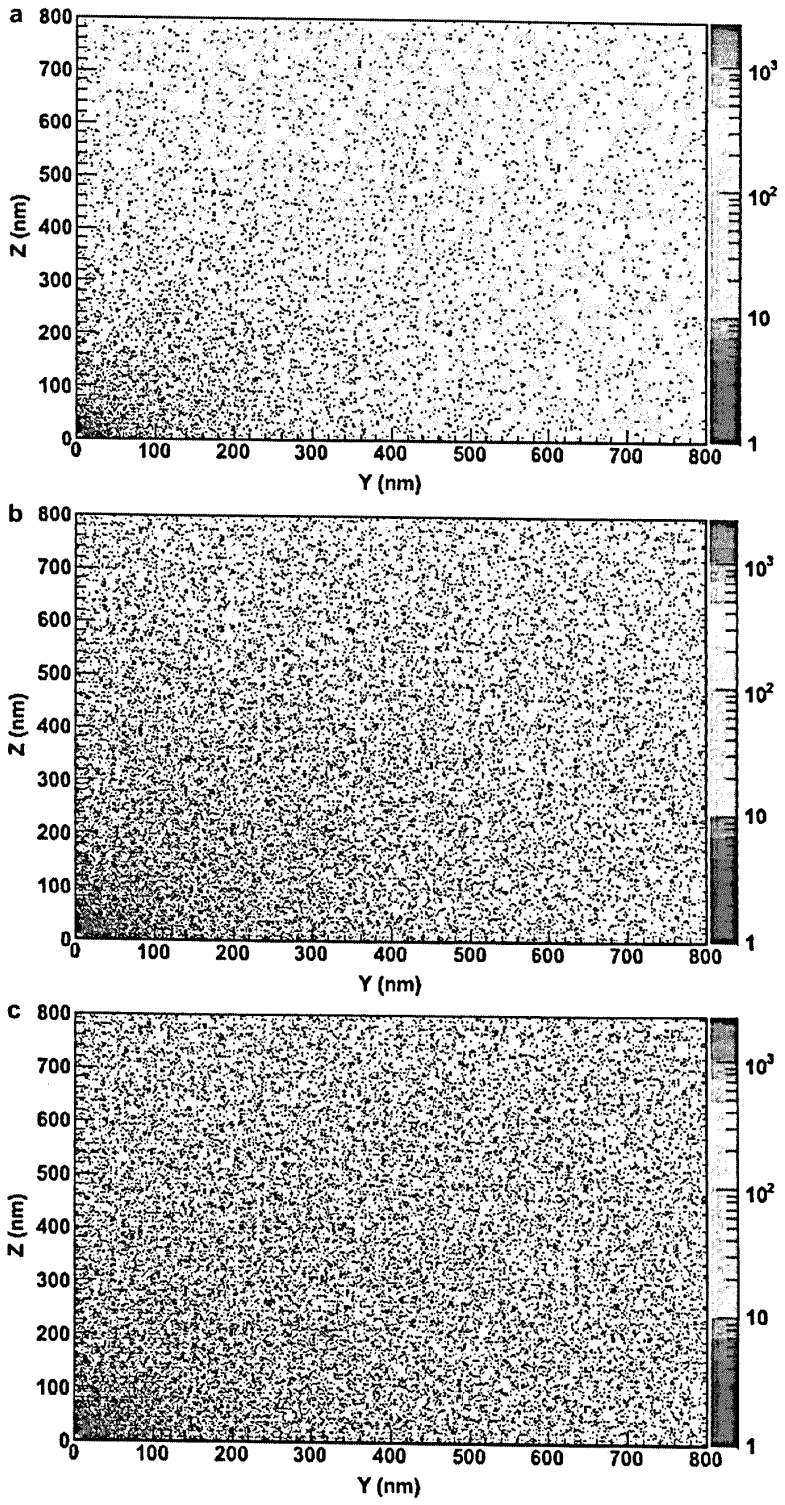

Figure 3. The distribution of ionisation clusters at different points along the trajectory of a 20 MeV proton pencil beam in the YZ plane, for slices of thickness 5 nm, for 2.0×10^4 incident protons. The colour scale on the right of each plot indicates the ionisation cluster size (number of ionisations per voxel). The beam is centred on (0,0). The top plot is for a depth of 0.0 mm in the water phantom and the middle and bottom plots are for depths 0.2 mm and 0.4 mm, respectively.

the entire phantom volume with 1.0×10^8 incident photons and 2.0×10^4 incident protons. However, the distribution of the ionisations within the phantom volume differs for each beam type.

For each particle type, the overall number of ionisations increases with beam depth in the phantom. The highest numbers of ionisations are concentrated in the vicinity of the beam for all planes.

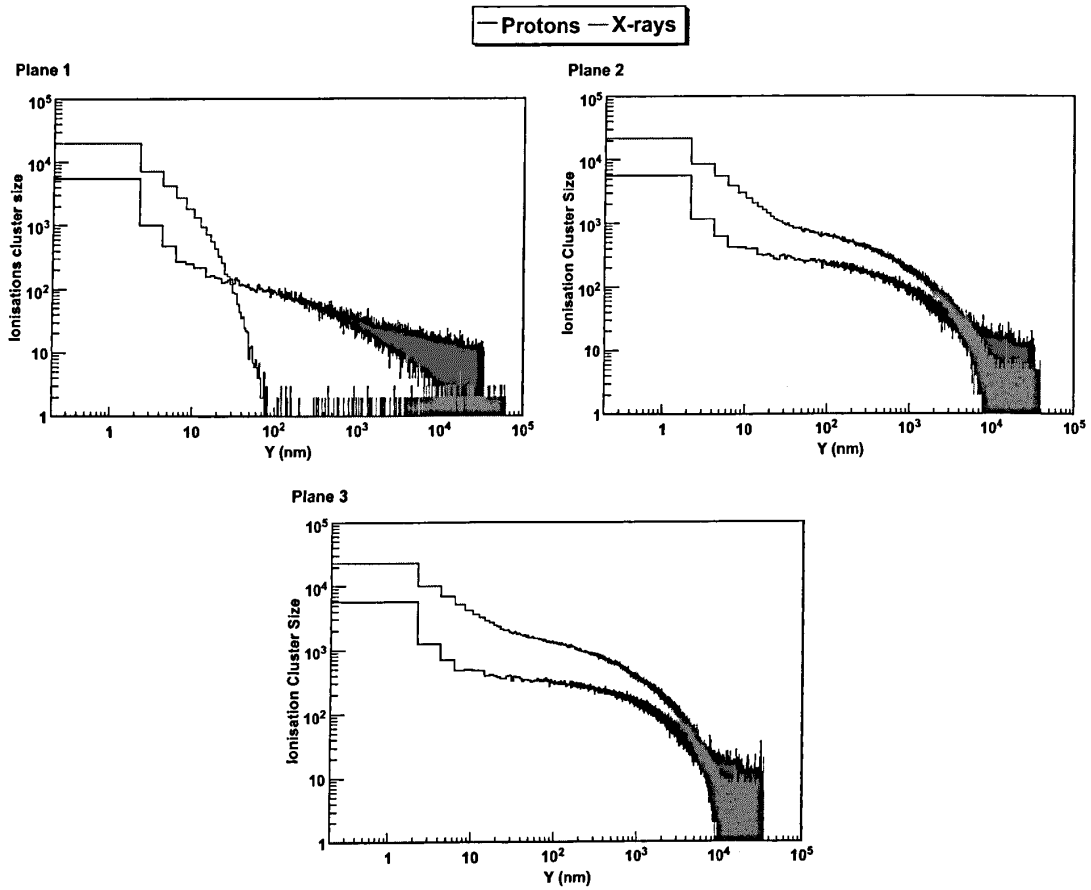

Figure 4. The number of ionisations (ionisation cluster size) within each nanometer-sized voxel (2 × 2 nm) at three different points along the beam trajectory for 10^8 incident 100 keV X-rays (red curve) and 2.0×10^4 incident 20 MeV protons (black curve). The beam is centred at 0 and plane 1 is at a depth of 0.0 mm, plane 2 at a depth of 0.2 mm and plane 3 at a depth of 0.4 mm.

The ionisation cluster distribution in plane 1 (Figure 2a and 3a) differs significantly between protons and X-rays. Few ionisations are formed adjacent to the beam path in the case of photons. However, in the proton case a substantial amount of ionisations are formed adjacent to the beam path in plane 1 (see Figure 4). Since the mass attenuation coefficient for 100 keV photons in liquid water is $\sim 1.707 \times 10^{-1}$ cm^2/g (Hubbell and Seltzer 2002, the scattering of photons will mostly occur at larger depths in the phantom, implying that ionisations will be formed within or close to the beam axis at small depths. The mean free path for ionisations in the case of 20 MeV protons is much less, ~ 0.03 μm (Villagrasa et al. 2011), and ionisations are formed in the first plane of the phantom.

At depths of 0.2 and 0.4 mm, photon scattering increases. This is evident by the larger distribution of ionisations in plane 2 and 3 (Figure 2b, 2c). Figure 4 clearly shows that photons have a higher number of ionisations, up to ~1 μm from the beam centre, than protons in plane 2 and 3. For each particle simulation, the overall number of ionisations within the entire phantom volume is constant, thus the proton ionisation cluster distribution extends to larger distances (>1000 nm) than the photon case. Ionisation clustering is concentrated closer to the photon beam centre than in the case for protons.

The radial dose distributions for the X-ray and proton beam are calculated in concentric rings from the beam centre (Figure 5). Each ring is 2 μm wide to allow for improved statistical accuracy. Photons deposit the highest dose in the vicinity of the beam centre. For photons, the difference in the distributed dose at different phantom depths is small with the highest dose occurring at a depth of 0.4 mm in the phantom (plane 3), coinciding with the region of highest ionisations. In the case of protons for planes 2 and 3, a large dose is deposited from the beam centre up to ~10^3 to 10^4 nm. While in the case of photons the dose decreases closer to the beam centre. At radii greater than ~1000 nm (less than an average cell size) from the beam centre, the dose profiles of the photon and proton beams show similarities, especially in plane 3. This indicates that at particular depths in the phantom the dose deposition of photons and protons can be similar. This however requires further investigation.

In summary, from this first study, we can infer that the cluster size and dose deposition distribution of a 20 MeV proton and a 100 keV photon are substantially different up to distances of a few micrometers from the centre of the beam (see Figure 4 and 5) and within plane 1. However in plane 2 and 3, at distances greater than ~ 1 μm (significantly smaller than the average cell size) the ionisation cluster size is

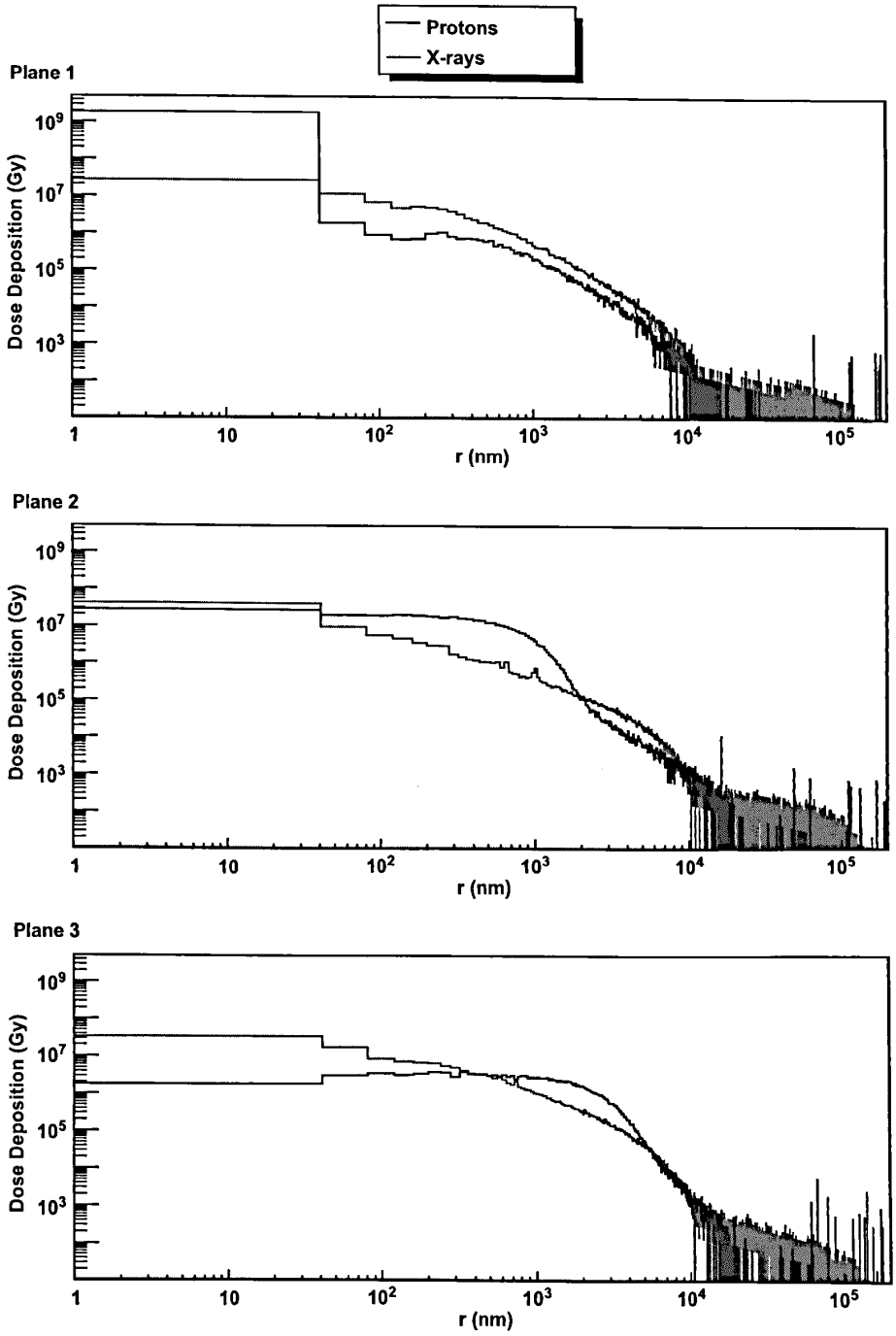

Figure 5. The radial dose distribution at three different positions along a 100 keV X-ray and 20 MeV proton pencil beam trajectory. The dose distribution is calculated in concentric rings for depths of 0.0 mm (top), 0.2 mm (middle) and 0.4 mm (bottom) in the cube phantom, for segments of thickness 2 μm.

approximately smaller than 100 for both particle beams, implying the beams will produce similar biological effects at this distance.

In conclusion, the results of this first study show that it may be feasible to substitute pencil beams of protons with X-rays in the case of a few cells, e.g., monolayer cell survival experiments, since the beams have similar characteristics at distances of few micrometers from the beam centre. In the case of uniformly distributed cells, e.g., small animal experiments, the beam profiles show significant differences at different depths along the beam track and substitution does not seem viable. Further investigation is however required to isolate the energies and depths at which proton and photon beams have equivalent properties on the nanometre scale.

Acknowledgements

Aimee McNamara would like to thank a travel grant provided by the Contributing to Australian Scholarship and Science

(CASS) Foundation to attend the MC2010 international workshop hosted by the Karolinska Institutet at the Royal Swedish Academy of Sciences, Stockholm, Sweden.

Declaration of interest

The authors report no conflicts of interest. The authors alone are responsible for the content and writing of the paper.

References

Agostinelli S, Allison J, Amako K, Apostolakis J, Araujo H, Arce P, Asai M, Axen D, Banerjee S, Barrand G, Behner F, Bellagamba L, Boudreau J, Broglia L, Brunengo A, et al. 2003. Geant4: A simulation toolkit. Nuclear Instruments and Methods A 506:250-303.

Allison J, Amako K, Apostolakis J, Araujo H, Dubois PA, Asai M, Barrand G, Capra R, Chauvie S, Chytracek R, Cirrone GAP, Cooperman G, Cosmo G, Cuttone G, Daquino GG, et al. 2006. Geant4 developments and applications. IEEE Transactions on Nuclear Science 53:270-278.

Brenner DJ, Ward JF. 1992. Constraints on energy deposition and target size of multiply damaged sites associated with DNA double-strand breaks. International Journal of Radiation Biology 61:737-748.

Champion C, Incerti S, Aouchiche H, Oubaziz D. 2009. A free-parameter theoretical model for describing the electron elastic scattering in water in the Geant4 toolkit. Radiation Physics and Chemistry 78:745-750.

Chauvie S, Francis Z, Guatelli S, Incerti S, Mascialino B, Montarou G, Moretto P, Nieminen P, Pia MG. 2006. Monte Carlo simulation of interactions of radiation with biological systems at the cellular and DNA levels: The Geant4-DNA project. Radiation Research 166:652-689.

Chauvie S, Francis Z, Guatelli S, Incerti S, Mascialino B, Moretto P, Nieminen P, Pia MG. 2007a. Geant4 physics processes for microdosimetry simulation: Design foundation and implementation of the first set of models. IEEE Transactions in Nuclear Science 54(6):2619-2628.

Chauvie S, Incerti S, Moretto P, Pia MG, Seznec H. 2007b. Microdosimetry in high-resolution cellular phantoms using the very low energy electromagnetic extension of the Geant4 toolkit. IEEE Nuclear Science Symposium Conference Record, N40-5:2086-2088.

Friedland W, Jacob P, Paretzke HG, Stork T. 1998. Monte Carlo simulation of the production of short DNA fragments by low-linear energy transfer radiation using higher-order DNA models. Radiation Research 150:170-182.

Hubbell JH, Seltzer SM. 2004. Tables of X-ray mass attenuation coefficients and mass energy-absorption coefficients (version 1.4). Accessed 18 April 2011 from the website: http://physics.nist.gov/xaamdi. Gaithersburg, MD: National Institute of Standards and Technology.

Incerti S, Seznec H, Simon M, Barberet P, Habchi C, Moretto P. 2009. Monte Carlo dosimetry for targeted irradiation of individual cells using a microbeam facility. Radiation Projection Dosimetry 133:2-11.

Miller DW. 1995. A review of proton beam radiation therapy. Medical Physics 22:1943-1955.

Nikjoo H, Goodhead DT. 1991. Track structure analysis illustrating the prominent role of low-energy electrons in radiobiological effects of low-LET radiations. Physics in Medicine and Biology 36:229-238.

Nikjoo H, O'Neill P, Goodhead DT, Terrissol M. 1997. Computational modelling of low-energy electron-induced DNA damage by early physical and chemical events. International Journal of Radiation Biology 71:467-483.

Nikjoo H, Uehara S, Wilson WE, Hoshi M, Goodhead DT. 1998. Track structure in radiation biology: Theory and applications. International Journal of Radiation Biology 73:355-364.

Nikjoo H, O'Neill P, Terrissol M, Goodhead DT. 1999. Quantitative modelling of DNA damage using Monte Carlo track structure method. Radiation and Environmental Biophysics 38:31-38.

Olsen DR, Bruland ØS, Frykholm G, Norderhaug IN. 2007. Proton therapy - a systematic review of clinical effectiveness. Radiotherapy and Oncology 83:123-132.

Siegbahn EA, Stepanek J, Brauer-Krisch E, Bravin A. 2006. Determination of dosimetrical quantities used in microbeam radiation therapy (MRT) with Monte Carlo simulations. Medical Physics 33: 3248-3260.

Spiga J, Siegbahn EA, Brauer-Krisch E, Randaccio P, Bravin A. 2007. The GEANT4 toolkit for microdosimetry calculations: Application to microbeam radiation therapy (MRT). Medical Physics 34: 4322-4331.

Villagrasa C, Francis Z, Incerti S. 2011. Physical models implemented in the Geant4-DNA extension of the Geant4 toolkit for calculating initial radiation damage at the molecular level. Radiation Protection Dosimetry 143:214-218.